Received: 3 February 2021 | Revised: 9 May 2021 | Accepted: 19 May 2021

DOI: 10.1111/cas.14995

ORIGINAL ARTICLE

Cancer Science WILEY

CCL23 suppresses liver cancer progression through the CCR1/AKT/ESR1 feedback loop

Jin Meng[1] | Lianghai Wang[1,2] | Jun Hou[1,2] | Xiaofeng Yang[1] | Ke Lin[1] | Hongxing Nan[1] | Man Li[1] | Xiangwei Wu[1,2] | Xueling Chen[1,2]

[1]Key Laboratory of Xinjiang Endemic and Ethnic Diseases/The First Affiliated Hospital, Shihezi University School of Medicine, Shihezi, China

[2]NHC Key Laboratory of Prevention and Treatment of Central Asia High Incidence Diseases, The First Affiliated Hospital, Shihezi University School of Medicine, Shihezi, China

Correspondence
Lianghai Wang, Xiangwei Wu and Xueling Chen, Key Laboratory of Xinjiang Endemic and Ethnic Diseases/the First Affiliated Hospital, Shihezi University School of Medicine, Shihezi, China.
Email: lh_wang@shzu.edu.cn (L.W.); wxwshz@126.com (X.W.); chenxueling@shzu.edu.cn (X.C.)

Funding information
Youth Innovation Talents Project of Shihezi University, Grant/Award Number: CXBJ201907; Science and Technology Cooperation Program of Xinjiang Production and Construction Corps, Grant/Award Number: 2021BC002; Youth Science and Technology Innovation Leading Talents Project of Xinjiang Production and Construction Corps, Grant/Award Number: 2020CB015; Non-profit Central Research Institute Fund of Chinese Academy of Medical Sciences, Grant/Award Number: 2020-PT330-003; National Natural Science Foundation of China, Grant/Award Number: 82060513, 82060297, 82060579 and 81902850

Abstract

With the ability to activate certain signaling pathways, chemokines and their receptors may facilitate tumor progression at key steps, including proliferation, immunomodulation, and metastasis. Nevertheless, their prognostic value and regulatory mechanism warrant thorough studies in liver cancer. Here, by screening the expression profiles of all known chemokines in independent liver cancer cohorts, we found that CCL23 was frequently downregulated at mRNA and protein levels in liver cancer. Decreased CCL23 correlated with shortened patient survival, enrichment of signatures related to cancer stem cell property, and metastatic potential. In addition to serving as a tumor suppressor through recruiting $CD8^+$ T cell infiltration in liver cancer, CCL23 could repress cancer cell proliferation, stemness, and mobility. Mechanistically, the expression of CCL23 was transcriptionally regulated by ESR1. On the other hand, CCL23 could suppress the activation of AKT signaling and thus promote the expression of ESR1, forming a feedback loop in liver cancer cells. Collectively, these findings reveal that loss of CCL23 drives liver cancer progression by coordinating immune evasion and metastasis initiation. Targeting the ESR1/CCL23/CCR1/AKT regulatory axis could be an effective therapeutic strategy.

KEYWORDS

chemokine, hepatocellular carcinoma, immune infiltration, metastasis, tumor suppressor

Abbreviations: ELISA, enzyme-linked immunosorbent assay; GSEA, gene set enrichment analysis; HCC, hepatocellular carcinoma; TCGA-LIHC, The Cancer Genome Atlas Liver Hepatocellular Carcinoma.

Jin Meng and Lianghai Wang contributed equally to this work.

1 | INTRODUCTION

Liver cancer is one of the most commonly diagnosed cancers and the leading cause of cancer death, with a heterogeneous prognosis depending on the etiology, geographical location, and stage of the disease at presentation.[1,2] Hepatocellular carcinoma (HCC) is mainly driven by chronic hepatitis B virus or hepatitis C virus infection, alcohol abuse, and several metabolic diseases.[3] Although HCC progression is considered a multistep and long-term progressive process, the precise molecular mechanism of HCC pathogenesis remains largely unknown.[4] Therefore, it is of great importance to explore novel tumor regulators and the underlying mechanisms of tumor metastasis that may provide new biomarkers for early diagnosis and new therapeutic targets for treatment in HCC.

Chemokines are a multigene family of small, secreted cytokines mediating cell migration during inflammation, immune surveillance, and organogenesis.[5,6] Chemokine subfamilies have been classified by the distance between the first two conserved cysteine residues, with the CXC and the CC subfamily containing the vast majority of all chemokines.[7] Although chemokines were initially characterized as attractants of leukocytes, it is now widely recognized that many cell types can express chemokines and chemokine receptors.[8-11] Chemokines have also been implicated in cellular transformation, tumor growth, invasion, homing of metastasis to distant sites, and host-tumor response. For instance, upregulation of CCL2 expression is correlated with clinical stage, overall survival, and macrophage infiltration in clear cell renal cell carcinoma.[12] CCL5 is found to be upregulated in ovarian cancer and contributes to the invasive capacity of ovarian cancer cells.[13] CCL14 is downregulated in HCC tumor tissues and associated with a poor prognosis.[14] CXCL8 overexpression in androgen-independent prostate cancer cells induces expression of MMP9, leading to increased local invasion of tumors.[15] With the ability to activate certain signaling pathways, chemokines and their receptors may facilitate tumor progression at key steps, including proliferation, immunomodulation, and metastasis.[16-18] Therefore, chemokines have attracted much attention, and their prognostic value and regulatory mechanism warrant thorough studies in liver cancer.

In this study, we explored the expression profiles of all known chemokines to screen out the chemokines associated with liver cancer progression. Data from bioinformatics analysis, cell lines, and clinical samples comprehensively characterized a novel mechanism by which an ESR1/CCL23/CCR1/AKT feedback loop collaboratively inhibits HCC progression.

2 | MATERIALS AND METHODS

2.1 | Data mining

The GEPIA 2 (http://gepia2.cancer-pku.cn/) was employed to compare the expression of chemokines between tumor and matched normal data in The Cancer Genome Atlas Liver Hepatocellular Carcinoma (TCGA-LIHC) with the default cutoff (|Log2FC| ≥1 and q-value ≤0.01). Association of chemokines on overall and disease-free survival was determined based on gene expression using median or quartile values as the cutoff. Disease-centric ESTIMATE results, including immune and ESTIMATE scores for liver HCC, were obtained from https://bioinformatics.mdanderson.org/estimate/disease.html?liver%20hepatocellular%20carcinoma_RNAseqV2. Immune subtypes consisting of C1 (wound healing), C2 (IFN-γ dominant), C3 (inflammatory), C4 (lymphocyte depleted), C5 (immunologically quiet), and C6 (TGF-b dominant) were obtained from the supplemental information of a previous immunogenomic analysis.[19] CIBERSORT immune fractions were obtained from https://gdc.cancer.gov/about-data/publications/panimmune. Correlations between CCL23 expression and $CD8^+$ T cell infiltration levels in TCGA-LIHC were explored using TIMER2.0 (http://timer.comp-genomics.org/). Gene set enrichment analysis (GSEA) was performed to search for the enrichment of pathways that may be regulated by CCL23 gene expression in TCGA-LIHC. Two additional publicly available liver cancer microarray datasets were downloaded from the Gene Expression Omnibus. GSE45267 contains gene expression profiles of 48 primary HCC samples and 39 noncancerous tissues. GSE14520 (platform GPL3921) analyzed gene expression patterns in 225 hepatitis B virus-related HCC samples and 220 nontumor tissues.

2.2 | Cell culture and transfection

Authenticated Hep3B, HepG2, Huh7, and SNU387 cells were obtained from the Cell Bank of the Chinese Academy of Sciences. Cells were cultured in Dulbecco's Modified Eagle Medium (DMEM) supplemented with 10% fetal bovine serum (Gibco) at 37°C with 5% CO_2 in an incubator. Lentivirus overexpressing CCL23 and siRNAs targeting CCL23 and ESR1 were purchased from GenePharma. Plasmid overexpressing ESR1 was obtained from Genechem. siRNAs and plasmid were transfected using Lipofectamine 3000 Transfection Reagent (Invitrogen) according to the manufacturer's instructions. All experiments were performed with mycoplasma-free cells.

2.3 | Real-time PCR

cDNA was generated from extracted total RNA by the RevertAid First Strand cDNA Synthesis Kit (Thermo Scientific). Quantification of gene expression was performed on a CFX96 Touch Real-Time PCR Detection System (Bio-Rad) with specific primers: CCL23 forward, AGATGACCCTTTCTCATGCTGC; CCL23 reverse, CTCTCCAGGAGTGAACACGG; ESR1 forward, AAAGG TGGGATACGAAAAGACC; ESR1 reverse, AGCATCCAACAAG GCACTGA; GAPDH forward, ACAACTTTGGTATCGTGGAAGG; GAPDH reverse, GCCATCACGCCACAGTTTC.

2.4 | Enzyme-linked immunosorbent assay

Cell culture supernatants from liver cancer cells were harvested for detecting CCL23 secretion by the Human CCL23 enzyme-linked

immunosorbent assay (ELISA) Kit (abcam #ab100611) according to the manufacturer's instructions.

2.5 | Cell proliferation assay

Different groups of cells were plated in clear-bottom 96-well plates. Cell proliferation was measured using Cell Counting Kit-8 (CCK-8; Dojindo) according to the manufacturer's instructions, and the absorbance was quantified at 450 nm (OD_{450}) with the Varioskan LUX Multimode Microplate Reader (Thermo Scientific).

2.6 | Hepatosphere formation assay

Single-cell suspensions were plated at 2×10^3 cells/well in 24-well ultralow-attachment plates. The seeded cells were propagated in serum-free DMEM/F12 medium supplemented with 20 ng/mL epidermal growth factor, 20 ng/mL fibroblast growth factor, and 2% B27. The growth of hepatospheres, namely the number and size, was measured after 10-day culture under a microscope.

2.7 | Cell migration and invasion assays

Cell migration assay was performed in 24-well plates with 8.0-μm-pore polycarbonate membrane inserts (Corning). Hep3B, Huh7, or SNU387 cells were seeded in the upper chamber in serum-free DMEM. The lower chamber was filled with DMEM and 10% fetal bovine serum. Hep3B and Huh7 cells were allowed to migrate for 48 hours, while SNU387 cells for 24 hours. Nonmigrant cells on the upper surface of the inserts were detached using a cotton swab. Filters were fixed with 4% formaldehyde for 15 minutes at 4°C, and the cells located on the lower surface of the inserts were stained with 0.1% crystal violet for 20 minutes and counted under a light microscope in three random fields. The cell invasion assay was essentially the same as the migration assay, except that the membrane insert was coated with Matrigel (BD Biosciences).

2.8 | Western blot

Equal amounts of cell lysates were separated by sodium dodecyl sulfate–polyacrylamide gel electrophoresis, transferred to polyvinylidene difluoride membranes, and subjected to immunoprobing with specific antibodies against ESR1 (Sigma-Aldrich #HPA000450), CCL23 (abcam #ab171751), CCR1 (abcam #ab19013), AKT (Cell Signaling Technology #4691), phospho-Akt (p-Akt, Cell Signaling Technology #4060), and β-actin (Cell Signaling Technology # 3700). The signals were detected using the Immobilon western chemilum HRP Substrate (Millipore #WBKLS0050), and images were obtained by a fluorescence/chemiluminescence imaging system (Clinx ChemiScope).

2.9 | Human tissue samples

A total of 111 primary HCC samples and 97 peritumor tissues (90 matched pairs) were obtained from patients undergoing surgical excision without prior radiotherapy or chemotherapy at the First Affiliated Hospital, Shihezi University School of Medicine from 2012 to 2019. This study was approved by the Ethics Committee of the First Affiliated Hospital, Shihezi University School of Medicine, and informed consent was obtained from the patients.

2.10 | Immunohistochemistry

Paraffin sections were deparaffinized, dehydrated, and antigen retrieved. The sections were blocked by 5% goat serum for 1 hour to reduce nonspecific background staining and incubated with primary antibody against CCL23 (abcam #ab171751) or CD8 (ZSGB-BIO #ZA-0508) overnight at 4°C. Subsequently, the sections were rinsed with TBS, treated with 3% H_2O_2 to block endogenous peroxidase activity, incubated with horseradish peroxidase–conjugated secondary antibody, and visualized by using a DAB Kit (ZSGB-BIO #ZLI-9018). Immunostaining degree of each sample was scored based on staining intensity (intensity score: 0, no staining; 1, weak staining; 2, intermediate staining; 3, strong staining) and proportion of positive cells (extent score: 0, < 5%; 1, 5%-25%; 2, 26%-75%; 3, 75%-100%). The final immunoreactivity score of CCL23 expression for each case is the product of the intensity score and the extent score. The counts for $CD8^+$ T cells represent an average number of positively stained cells within three random intratumor areas under a 20X objective.

2.11 | Statistical analysis

Numerical data are presented as mean ± SEM. Statistical analyses were performed using GraphPad Prism 8. Comparison between groups was conducted using a Mann-Whitney test, Wilcoxon matched-pairs signed rank test, two-tailed Student's *t*-test, or ANOVA with post hoc tests. Kaplan-Meier analysis and log-rank test were used for survival estimates. The significance of association between genes was evaluated using Spearman's correlation. A *P*- value <.05 was considered statistically significant; $^*P < .05$, $^{**}P < .01$, $^{***}P < .001$.

3 | RESULTS

3.1 | CCL23 is downregulated in liver cancer and correlates with poor prognosis

To screen out the chemokines associated with liver cancer progression, we explored the expression profiles of all known chemokines in the TCGA-LIHC cohort using the GEPIA 2 web server. Twelve chemokines were differentially expressed between the matched liver cancer and normal tissues (Table 1). Among them, the mRNA

expressions of CCL14, CCL19, CCL21, CCL23, CXCL2, CXCL12, and CXCL14 were significantly decreased, while the expressions of CCL15, CCL18, CCL20, CXCL9, and CXCL10 were significantly elevated in tumors compared with normal tissues (Figures 1A and S1A). To elucidate the prognostic significance of the above differentially expressed chemokines, survival analyses based on their expression status were further performed. Kaplan-Meier curves revealed that the low expression levels of CCL14, CCL23, and CXCL2 were significantly associated with decreased overall survival, while low CCL14, CCL21, and CCL23 were significantly correlated with shorter disease-free survival (Figures 1B, S2 and S3). In addition to liver cancer, the gene expression levels of CCL23, CCL14, CCL21, and CXCL2 were found to be also downregulated across multiple cancer types compared with their respective matched normal tissues (Figures 1G and S1B). Significantly reduced CCL23 expression levels in HCC compared with nontumor tissues were further validated in two independent case sets, GSE45267 and GSE14520 (Figure 1C,D). Kaplan-Meier analysis results showed that patients with low CCL23 expression also had shorter overall survival and recurrence-free survival in the GSE14520 dataset (Figure 1E). Moreover, low CCL23 expression was significantly correlated with advanced pathologic stage, higher histologic grade, and metastasis signature (Figure 1F). Collectively, the downregulated expression of CCL23 was associated with poor prognosis in liver cancer and was selected for further analysis.

3.2 | CCL23 is associated with immune infiltration in liver cancer

To determine the potential correlation between CCL23 expression and immune infiltration in liver cancer, the patients from TCGA-LIHC were first divided into high and low groups based on their immune score representing the infiltration of immune cells in tumor tissue or ESTIMATE score inferring tumor purity predicted by the ESTIMATE algorithm. Kaplan-Meier survival curves revealed that patients with high immune scores or ESTIMATE scores had a longer disease-free interval and progression-free interval compared with those with low scores (Figure 2A,B). The immune score was significantly higher in tumors with high CCL23 expression than that with low CCL23 (Figure 2C) and positively correlated with CCL23 expression levels (Spearman r = .417, P <.00001; Figure 2D). Six immune subtypes spanning cancer tissue types and molecular subtypes have been identified and hypothesized to define immune response patterns impacting patient prognosis.[19] Liver cancers with high CCL23 expression exhibited more C2 (IFN-γ dominant) and C3 (inflammatory) subtypes, which are supposed to have the most favorable prognosis and display a type I immune response. In contrast, the C4 (lymphocyte depleted) subtype, which is associated with the worst prognosis and immunosuppressed composite signatures reflecting low lymphocytic infiltrate and high M2 macrophage content, was enriched in CCL23-low tumors (Figure 2E). On the other hand, tumors in the C2 and C3 subtypes displayed significantly higher CCL23 expression levels (Figure 2F). The infiltration of 22 immune cell subgroups in liver cancer with differential CCL23 expression was further evaluated using the CIBERSORT algorithm. Results showed that $CD8^+$ T cells were significantly enriched in tumor tissues with higher CCL23 expression (Figure 2G). The positive correlation between CCL23 expression and $CD8^+$ T cell infiltration level was confirmed by the TIMER2.0 webserver (Figure 2H), suggesting that CCL23 might serve as a tumor suppressor through recruiting $CD8^+$ T cell infiltration in liver cancer.

TABLE 1 Tumor/normal tissue differentially expressed chemokines in TCGA-LIHC

Gene symbol	Median (tumor)	Median (normal)	Log2(fold change)	adj.p
CCL14	7.250	46.812	−2.535	1.04e-34
CCL15	29.421	9.305	1.562	1.09e-23
CCL18	2.040	0.510	1.010	1.72e-11
CCL19	2.700	8.890	−1.418	1.65e-6
CCL20	22.420	1.500	3.228	7.05e-19
CCL21	7.730	17.895	−1.114	1.21e-5
CCL23	0.220	2.155	−1.371	1.11e-67
CXCL2	18.181	119.784	−2.655	1.51e-45
CXCL9	4.180	0.765	1.553	5.77e-14
CXCL10	11.720	1.145	2.568	3.36e-23
CXCL12	11.660	60.325	−2.276	7.53e-40
CXCL14	0.190	14.215	−3.676	7.94e-78

Abbreviations: TCGA-LIHC, The Cancer Genome Atlas Liver Hepatocellular Carcinoma.

3.3 | CCL23 suppresses aggressive phenotypes in liver cancer cells

To further investigate the potential functions of CCL23 in liver cancer progression, we performed GSEA comparing CCL23-high and CCL23-low cancers from the TCGA-LIHC cohort (Figure 3A). Gene sets related to metastasis ("LIAO_METASTASIS" and "WINNEPENNINCKX_MELANOMA_METASTASIS_UP"), stem cell ("WONG_EMBRYONIC_STEM_CELL_CORE" and "OISHI_CHOLANGIOMA_STEM_CELL_LIKE_UP"), liver cancer cell cycle/proliferation ("BOYAULT_LIVER_CANCER_SUBCLASS_G3_UP" and "CHIANG_LIVER_CANCER_SUBCLASS_PROLIFERATION_UP"), and poor survival of HCC ("LEE_LIVER_CANCER_SURVIVAL_DN") were significantly enriched in the CCL23-low expression group. To further define the role of CCL23 in liver cancer cells, we evaluated the effect of CCL23 gain-of-function (Figure 3B,C). Ectopic expression of CCL23 in HepG2 cells significantly suppressed cell proliferation compared with the vector control (Figure 3D). Using the nonadherent hepatosphere formation assay, overexpression of CCL23, not the vector control, significantly decreased the hepatosphere number in HepG2 and Hep3B cells (Figure 3E). CCL23 overexpression also resulted in significant inhibition of cell migration ability in Hep3B, Huh7, and SNU387 cells

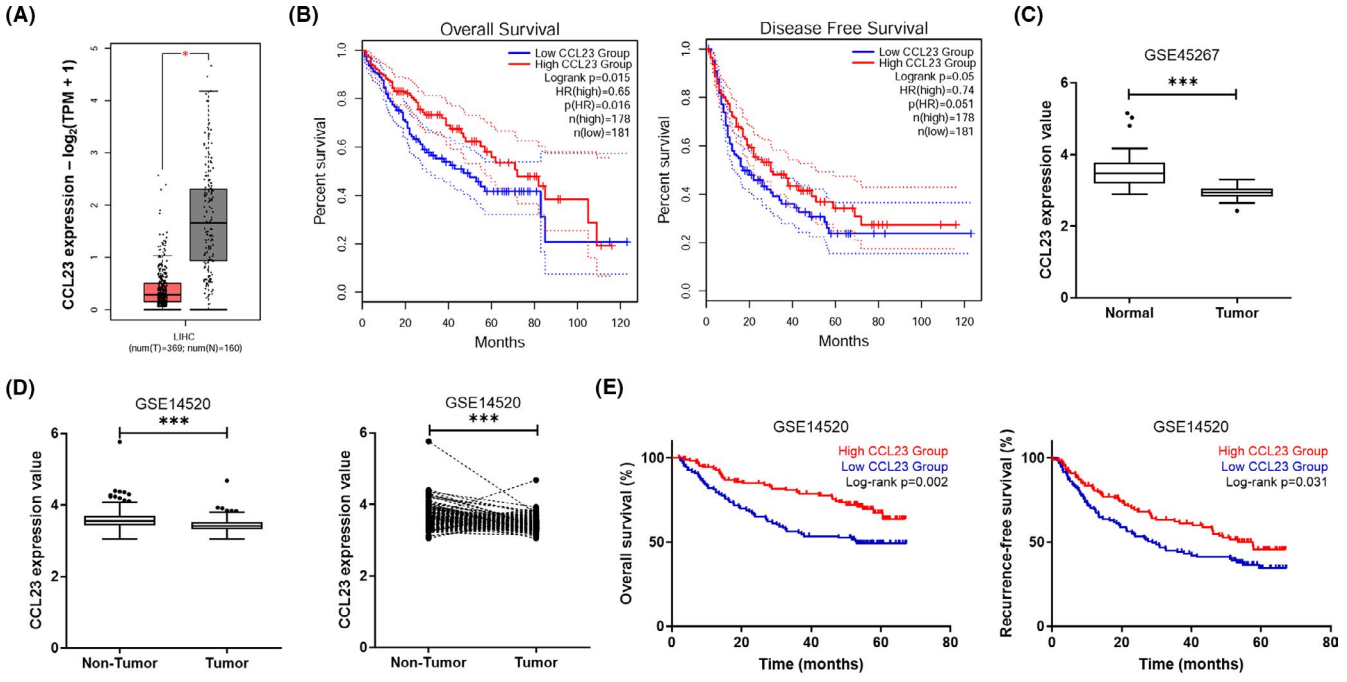

Dataset	Variable	CCL23 expression		*P* value	
		Low	High	χ2	Fisher
TCGA-LIHC	Pathologic stage				
	I/II	122	135	0.0407	0.0498
	III/IV	54	36		
	Neoplasm histologic grade				
	G1/2	99	133	0.0001	0.0001
	G3/4	85	49		
GSE14520	Predicted.risk.Metastasis.Signature				
	Low	48	66	0.0186	0.0222
	High	62	45		

FIGURE 1 CCL23 is downregulated in liver cancer and correlates with worse patient prognosis. A, Box plots comparing CCL23 expression between The Cancer Genome Atlas Liver Hepatocellular Carcinoma (TCGA-LIHC) tumor samples and matched TCGA normal and GTEx data. B, Kaplan-Meier analysis of CCL23 expression level and overall survival (left) or disease-free survival (right) of patients from TCGA-LIHC. C, Box plot showing CCL23 expression values in 48 primary hepatocellular carcinoma (HCC) samples and 39 noncancerous tissues from the GSE45267 dataset. D, The expression levels of CCL23 in 225 hepatitis B virus-related HCC and 220 nontumor tissues (left) or 213 paired tumor and nontumor tissues from the GSE14520 (GPL3921) dataset. E, Kaplan-Meier curves for overall survival (left) or recurrence-free survival (right) of liver cancer patients from the GSE14520 dataset according to CCL23 expression level. F, Correlation between CCL23 expression and clinicopathological features in liver cancer. G, Dot plot showing the CCL23 expression profile across all tumor samples and matched normal tissues. *P*-values determined by one-way ANOVA (A), Mann-Whitney test (C and D), or Wilcoxon matched-pairs signed rank test (D)

and invasive potential in SNU387 cells (Figure 3F,G). These observations indicate that CCL23 could repress liver cancer cell proliferation, stemness, and mobility.

3.4 | CCL23 is a transcriptional target of ESR1

To gain insight into the underlying mechanism of CCL23 loss in liver cancer, we first analyzed the genetic alterations of the CCL23 locus in the TCGA-LIHC dataset. Only one out of 372 liver cancer samples exhibited CCL23 deep deletion (Figure S4A). No correlation of CCL23 mRNA expression with its copy number status was found (Figure S4B). To figure out whether transcriptional regulation is involved in the decreased CCL23 expression in liver cancer, we assessed the tumor/normal tissue differentially expressed genes (obtained from the GEPIA 2) that significantly correlated with CCL23 expression (derived from the cBioPortal for Cancer Genomics) and then integrated them with the putative transcriptional factors which could regulate CCL23 transcription (predicted by the HumanTFDB[20]). Intriguingly, three candidates, including ESR1, CBX3, and MTA3, were identified. Among them, ESR1 expression was significantly downregulated in liver cancers and was positively correlated with CCL23 expression (Figure 4A,B). The low-ESR1 group exhibited shortened overall survival and disease-free survival (Figure 4C). In contrast, the

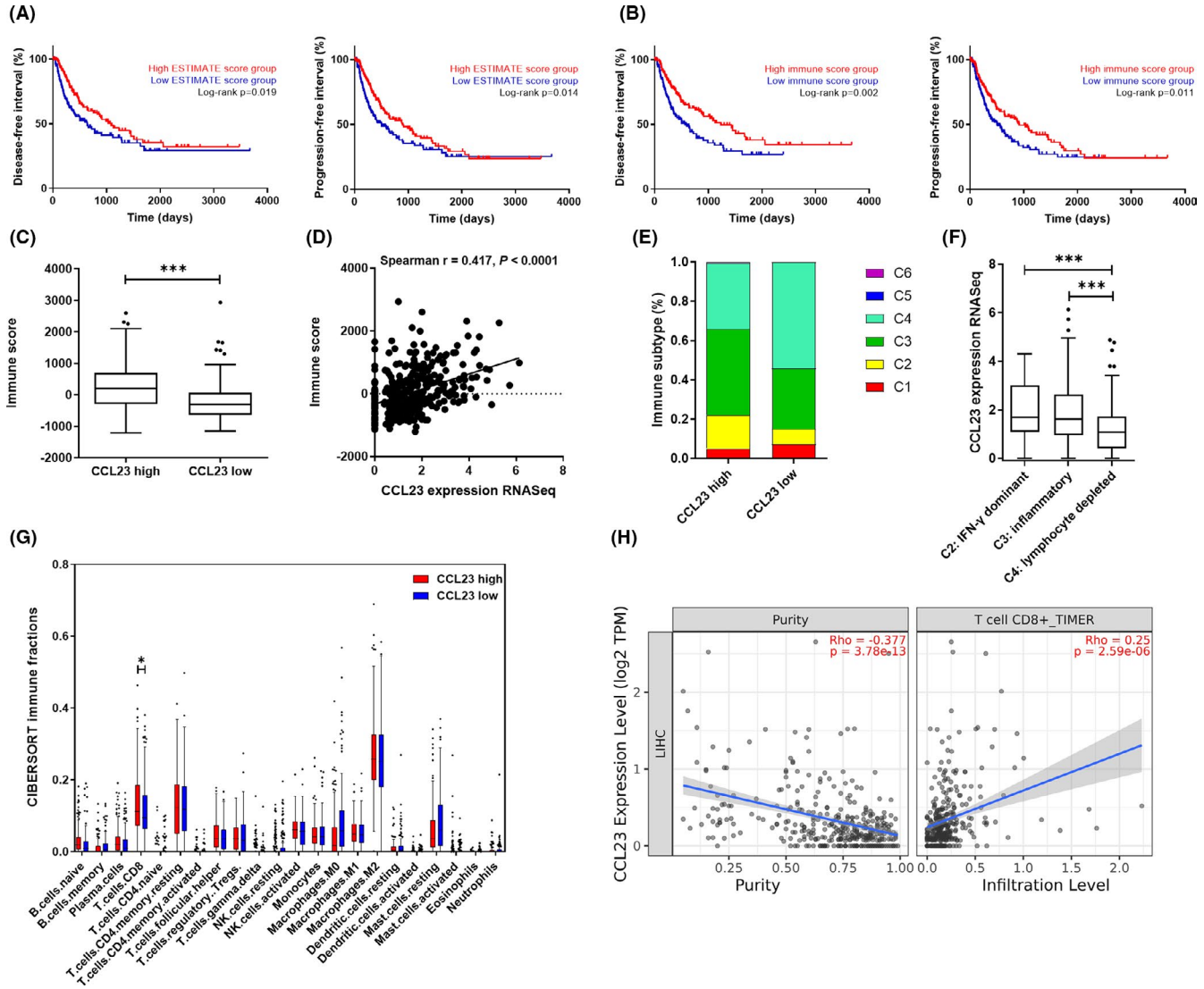

FIGURE 2 Correlation between CCL23 expression and immune infiltration in liver cancer. A, B, High immune score (A) or ESTIMATE score (B) was associated with prolonged disease-free interval (left) and progression-free interval (right) in patients from The Cancer Genome Atlas Liver Hepatocellular Carcinoma (TCGA-LIHC). C, Box plot comparing the immune score in CCL23-high and CCL23-low tumors. The cutoff value for high- vs. low-CCL23 groups was set at the median. D, Scatterplot showing the correlation between CCL23 expression and immune score in the TCGA-LIHC cohort. E, Distribution of six immune subtypes (C1-C6) within CCL23-high and CCL23-low tumors. F, Box plot comparing CCL23 expression levels in the indicated immune subtypes. G, CIBERSORT immune fractions of 22 subtypes of immune cell infiltration in liver cancers with high and low CCL23 expression levels. H, Scatter plots presenting the correlation between CCL23 expression level and the purity-adjusted $CD8^+$ T cell infiltrates estimation value in TCGA-LIHC. *P*-values determined by Mann-Whitney test (C and G) or one-way ANOVA with Tukey's multiple comparison test (F)

expression of CBX3 and MTA3 was markedly increased in tumor samples and reversely correlated with CCL23 expression (Figure S4C-F). Patients in the high-CBX3 and high-MTA3 groups had poor overall survival and disease-free survival (Figure S4G-H). However, among these candidate transcriptional factors, a significant correlation with CCL23 expression was only identified for ESR1 (ESR1 overexpression significantly enhanced CCL23 mRNA level in HepG2 and SNU387 cells, while ESR1 interference abolished CCL23 expression in Hep3B cells), but not for CBX3 and MTA3 (Figures 4D,E and S4I). Analysis of publicly available datasets identified ESR1-binding peaks associated with the CCL23 gene locus in cancer cells of the prostate and breast (Figure 4F). At the functional level, ectopic expression of ESR1 significantly suppressed hepatosphere-forming capacity in HepG2 and Hep3B cells (Figure 4G). Conversely, the inhibitory effect of ESR1 on cell migration was reversed by silencing CCL23 expression or treatment with BX471, a CCR1-specific antagonist, in Hep3B and SNU387 cells (Figure 4H,I).

3.5 | CCL23 inhibits the AKT signaling and forms a CCR1/AKT/ESR1 feedback loop

To further explore the downstream mechanism of CCL23 inhibiting liver cancer progression, we dug ESR1/CCL23/CCR1-related

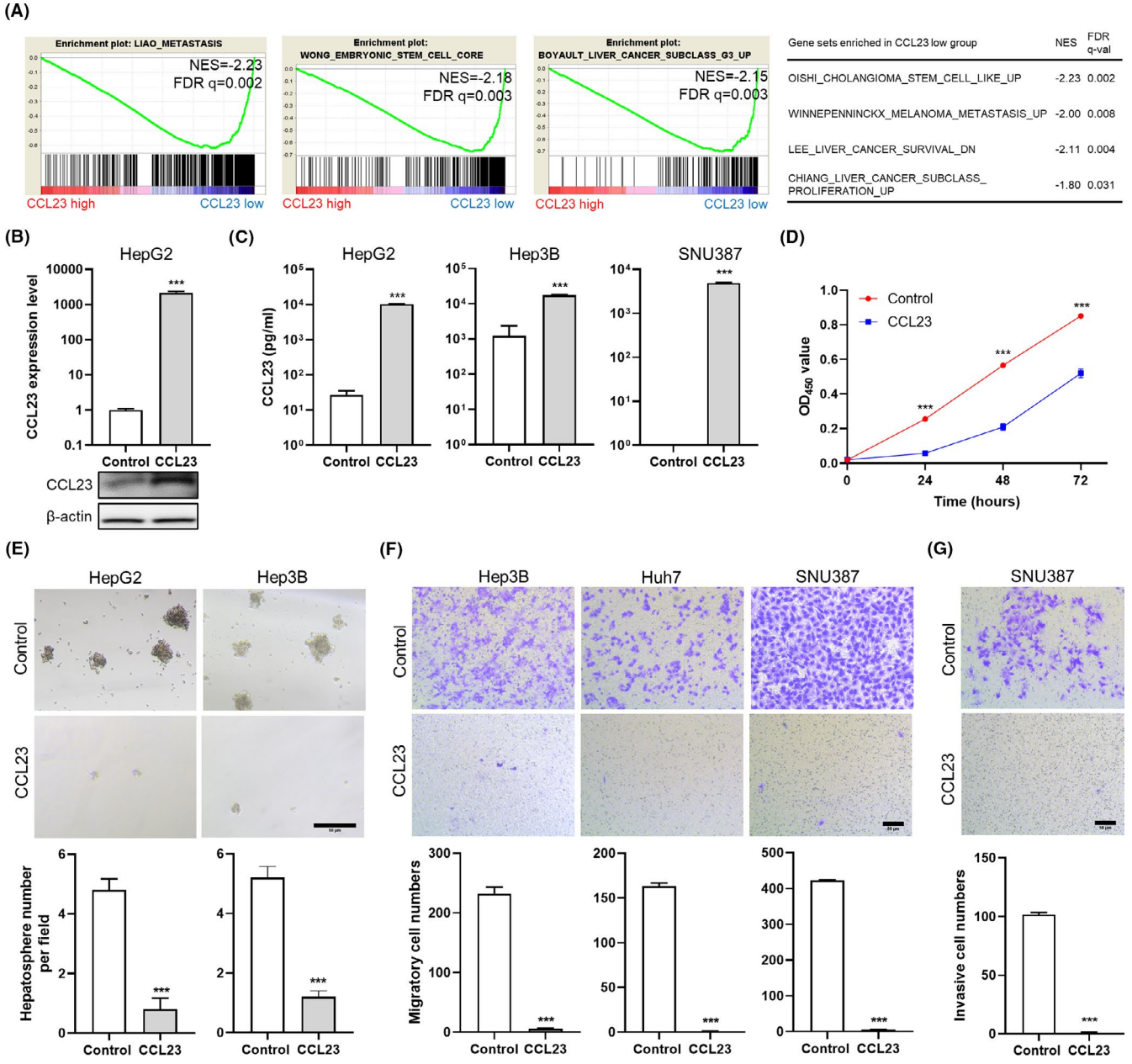

FIGURE 3 CCL23 antagonizes malignant phenotypes of liver cancer cells. A, Gene set enrichment analyses (GSEA) showing significant enrichment of the indicated gene sets comparing CCL23-high and CCL23-low cancers from The Cancer Genome Atlas Liver Hepatocellular Carcinoma (TCGA-LIHC) cohort. NES, normalized enrichment score. FDR, false discovery rate. B, Real-time PCR (up) and Western blotting (bottom) analysis confirming elevated CCL23 level in HepG2 cells after ectopic expression of CCL23. C, Liver cancer cells with CCL23 ectopic expression were incubated for 48 h. Secretion of CCL23 in the cell culture supernatants was measured by ELISA. D, Growth curves of HepG2 cells with CCL23 overexpression measured by CCK8 assay. E, Representative images (top) and quantification (bottom) of hepatospheres formed by HepG2 and Hep3B cells after CCL23 overexpression. F, Representative images (top) and quantification (bottom) of the indicated CCL23-overexpressing cells that migrated through the Transwell membrane. G, Representative images (left) and quantification (right) of CCL23-overexpressing SNU387 cells invaded through the Transwell membrane. *P*-values determined by two-way ANOVA (D) or unpaired two-tailed Student's *t*-test (E-G)

signaling cascades and chose AKT because it often played a role in promoting metastasis in various tumors.[21-23] Intriguingly, CCL23 marked abrogated AKT activation in Hep3B and HepG2 cells (Figure 5A). In contrast, blocking the CCL23 receptor with BX471 rescued the phosphorylation of AKT in CCL23-overexpressed cells. Moreover, treatment with MK-2206 2HCl, a highly selective AKT inhibitor, significantly reversed the enhancing effects of CCL23 knockdown on the migration capacity of Hep3B cells (Figure 5B), indicating that CCL23 functions through inhibiting AKT signaling.

Unexpectedly, we noticed that the expression of ESR1 was significantly decreased upon treatment with small interfering RNAs targeting CCL23 (siCCL23) in HepG2 cells (Figure 4D). This leads to the hypothesis that CCL23 could regulate the expression of ESR1 in some way and forms a feedback loop. Real-time analysis confirmed

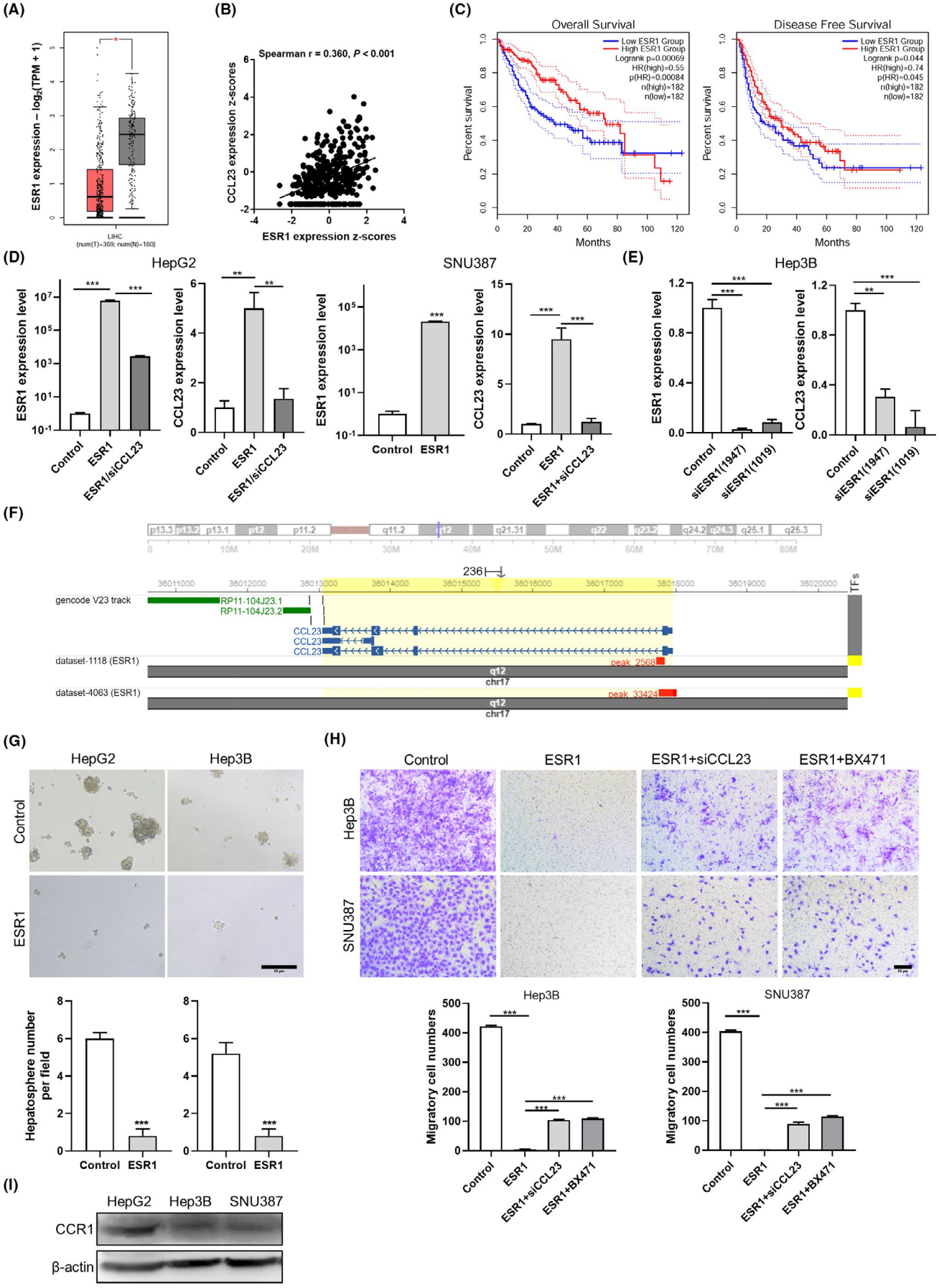
(A)
ESR1 expression – log2(TPM + 1)
LIHC
(num(T)=369; num(N)=160)
(B)
Spearman r = 0.360, P < 0.001
CCL23 expression z-scores
ESR1 expression z-scores
(C)
Overall Survival
Disease Free Survival
Low ESR1 Group
High ESR1 Group
Logrank p=0.00069
HR(high)=0.55
p(HR)=0.00084
n(high)=182
n(low)=182
Logrank p=0.044
HR(high)=0.74
p(HR)=0.045
Percent survival
Months
(D)
HepG2
SNU387
ESR1 expression level
CCL23 expression level
Control
ESR1
ESR1/siCCL23
ESR1+siCCL23
(E)
Hep3B
siESR1(1947)
siESR1(1019)
(F)
gencode V23 track
RP11-104J23.1
RP11-104J23.2
CCL23
dataset-1118 (ESR1)
peak_2568
dataset-4063 (ESR1)
peak_33424
chr17
TFs
(G)
HepG2
Hep3B
Control
ESR1
Hepatosphere number per field
(H)
Control
ESR1
ESR1+siCCL23
ESR1+BX471
Hep3B
SNU387
Migratory cell numbers
(I)
HepG2
Hep3B
SNU387
CCR1
β-actin

FIGURE 4 Transcriptional regulation of CCL23 expression by ESR1. A, Box plots comparing ESR1 expression between The Cancer Genome Atlas Liver Hepatocellular Carcinoma (TCGA-LIHC) tumor samples and matched TCGA normal data. B, Scatterplot showing the correlation between ESR1 expression and CCL23 expression in the TCGA-LIHC cohort. C, Kaplan-Meier curves for overall survival (left) or disease-free survival (right) of liver cancer patients based on ESR1 expression. D, Real-time PCR analysis of ESR1 and CCL23 expression levels after ESR1 overexpression in the presence or absence of small interfering RNAs targeting CCL23 (siCCL23) in HepG2 and SNU387 cells. E, The expression levels of ESR1 and CCL23 in Hep3B cells after treatment with small interfering RNAs targeting ESR1 (siESR1). F, Exploring and visualizing the ESR1 binding peaks on the CCL23 locus by using the hTFtarget database (http://bioinfo.life.hust.edu.cn/hTFtarget#!/). Dataset 1118 from prostate VcaP cells; dataset 4063 from breast cancer patient–derived xenograft. G, Representative images (top) and quantification (bottom) of hepatospheres formed by HepG2 and Hep3B cells after ESR1 overexpression. H, Representative images (top) and quantification (bottom) of ESR1-overexpressing cells in the presence or absence of siCCL23 or BX471 (10 μM) that migrated through the Transwell membrane. I, The expression of CCR1 in HepG2, Hep3B, and SNU387 cells was confirmed by Western blotting. β-actin was served as a loading control. *P*-values determined by one-way ANOVA (A, D, E, and H) or unpaired two-tailed Student's *t*-test (D and G)

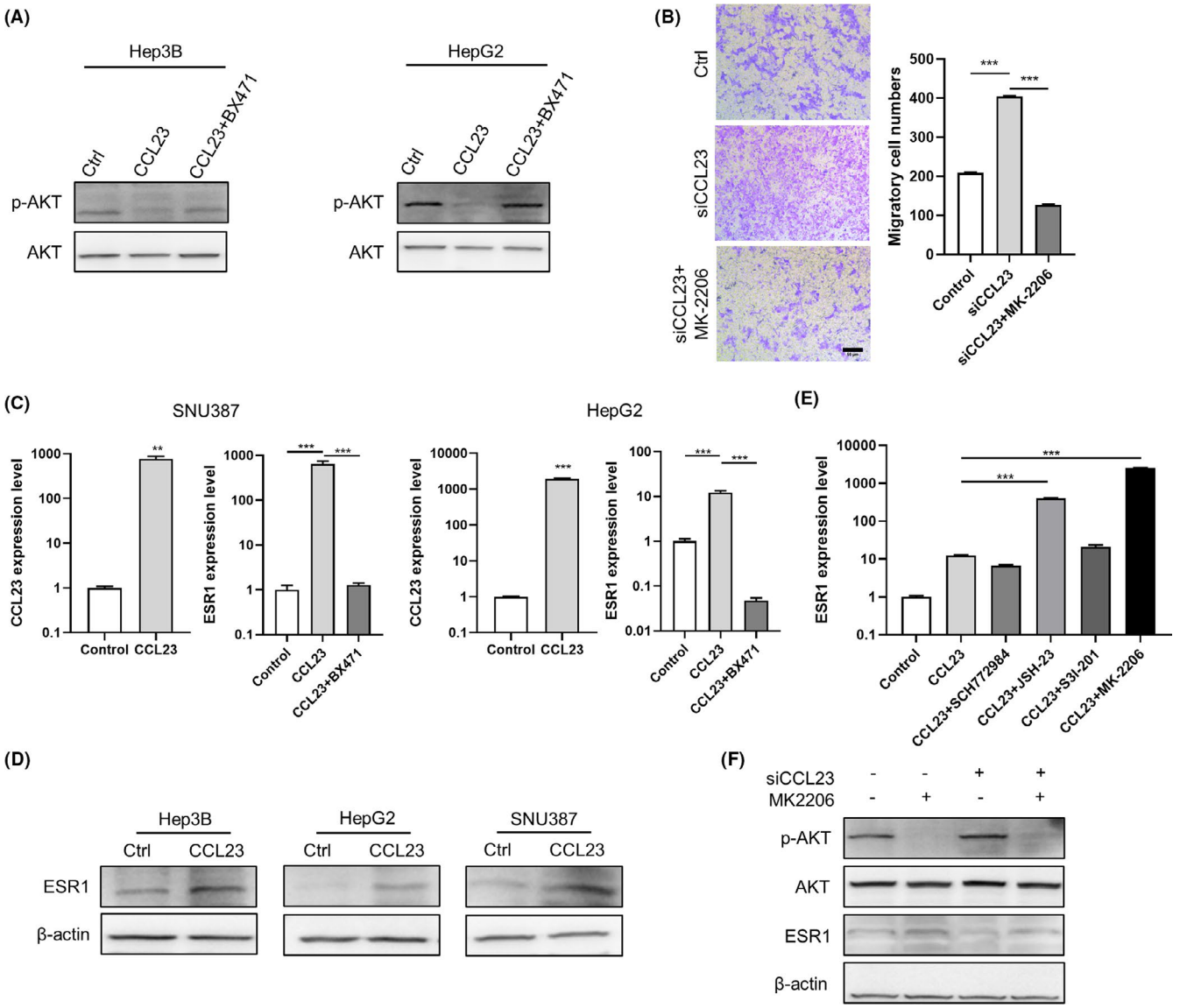

FIGURE 5 CCL23 functions through the CCR1/AKT/ESR1 feedback loop. A, After CCL23 overexpression and BX471 (10 μM) treatment, the activation status of AKT signaling was determined in Hep3B and HepG2 cells by Western blotting. B, Representative images (left) and quantification (right) of migratory Hep3B cells treated with siCCL23 and MK-2206 (10 μM) using Transwell assay. C, Real-time PCR analysis of CCL23 and ESR1 expression levels after CCL23 overexpression and BX471 (10 μM) treatment in SNU387 and HepG2 cells. D, Western blotting analysis of ESR1 level after ectopic expression of CCL23 in Hep3B, HepG2, and SNU387 cells. β-actin was used as a loading control. E, Real-time PCR analysis of ESR1 expression levels in the presence of SCH772984 (10 μM), JSH-23 (50 μM), S3I-201(100 μM), or MK-2206 (10 μM) in CCL23-overexpressed HepG2 cells. F, The activation status of AKT signaling and ESR1 expression levels after treatment with siCCL23 and MK-2206 (10 μM) were determined in HepG2 cells by Western blotting. *P*-values determined by one-way ANOVA (B, C, and E) or unpaired two-tailed Student's *t*-test (C)

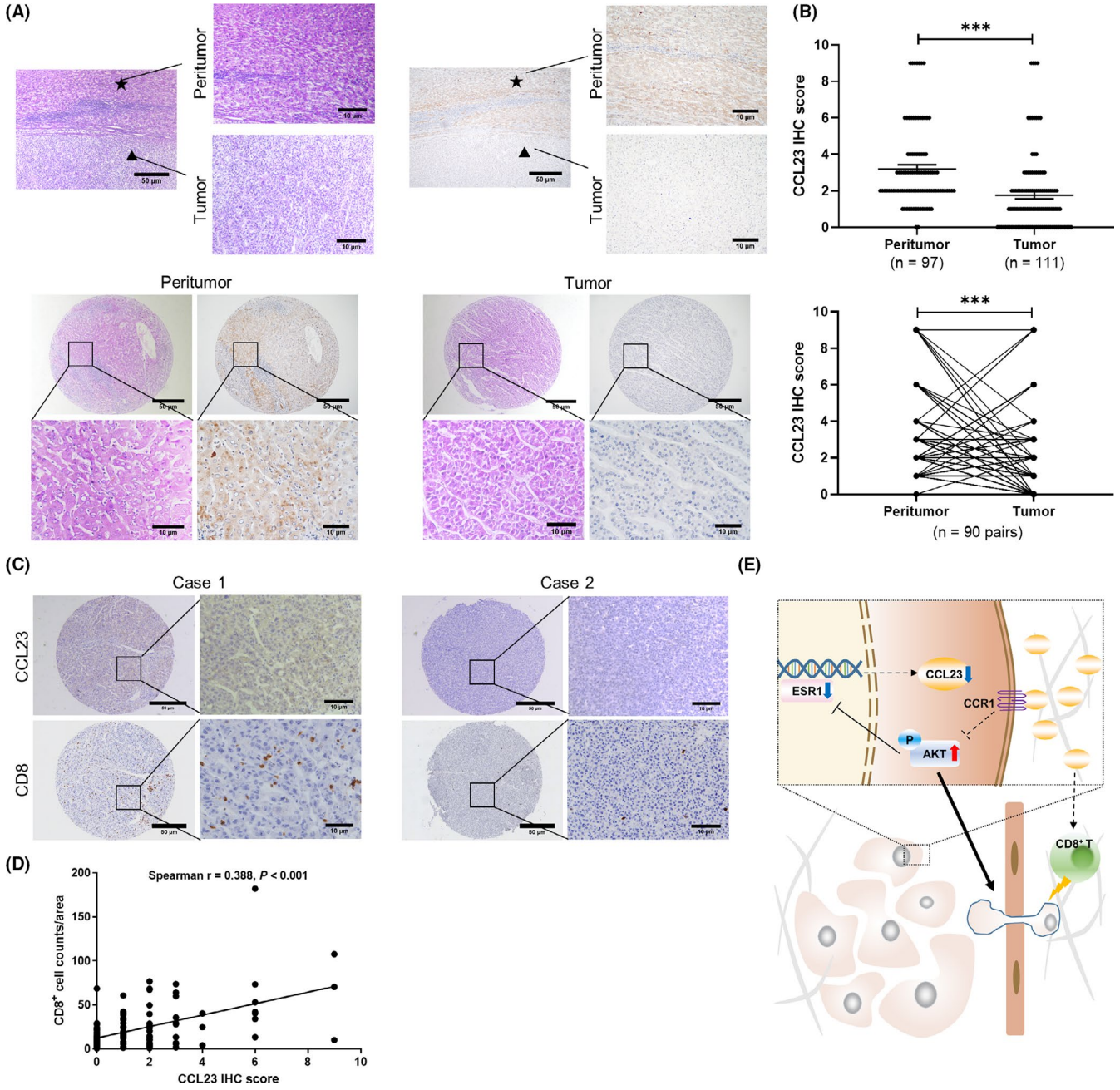

FIGURE 6 Underexpression of CCL23 in liver cancers at the protein level. A, Representative H&E and immunohistochemical staining of CCL23 expression in liver cancer and peritumor tissues. B, Statistical analysis of CCL23 immunohistochemistry scores in liver cancers and peritumor tissues (top) or paired tumor and peritumor tissues (bottom). *P*-values determined by Mann-Whitney test (top) and Wilcoxon matched-pairs signed rank test (bottom). C, Representative images of $CD8^+$ T cell infiltration in liver cancers with different CCL23 levels. D, Scatterplot representing the correlation between $CD8^+$ T cell infiltration and CCL23 immunohistochemistry scores. E, A proposed model for an ESR1/CCL23/CCR1/AKT regulatory circuit promotes tumor metastasis and inhibits $CD8^+$ T cell infiltration in liver cancer progression

that the ectopic expression of CCL23 promoted ESR1 expression, whereas cotreatment with BX471 to antagonize CCR1 abolished the CCL23-induced ESR1 expression in SNU387 and HepG2 cells (Figure 5C). Similarly, the protein levels of ESR1 were markedly increased after CCL23 overexpression in Hep3B, HepG2, and SNU387 cells (Figure 5D). To screen out the mediator connecting CCL23 and ESR1, we tested specific inhibitors of ERK1/2 (SCH772984), NF-κB nuclear translocation (JSH-23), STAT3 (S31-201), and AKT (MK-2206 2HCl). Of note, MK-2206 exhibited the most prominent enhancement of ESR1 expression in CCL23-overexpressed HepG2 cells (Figure 5E), consistent with the previous observation that the activation of AKT could inactivate FOXO3A, leading to reduced transcription of ESR1 (encoding ERα) in breast cancer cells.[24,25] In line with these data, interference of CCL23 increased AKT phosphorylation and decreased ESR1 protein level, whereas inhibition of AKT by MK-2206 in siCCL23-treated HepG2 cells rescued the expression of ESR1 protein (Figure 5F). These results suggest a CCL23/CCR1/AKT/ESR1 feedback loop in liver cancer cells.

3.6 | CCL23 is underexpressed in liver cancers at the protein level

To further investigate the clinical significance of decreased CCL23 expression in liver cancer, we assessed the expression pattern of CCL23 at the protein level using immunohistochemistry staining in a tissue microarray. Results showed that the mean immunoreactivity scores of CCL23 in liver cancer were significantly lower than those in the peritumor samples. CCL23 staining was also apparently weaker in liver cancer regions than their paired nontumor tissues (Figure 6A,B). We further stained CD8 to evaluate the $CD8^+$ T cell infiltration in the same series of tumors. Consistent with the findings speculated by bioinformatics, we revealed a positive association of $CD8^+$ T cell infiltration with CCL23 immunoreactivity scores (Figure 6C,D).

4 | DISCUSSION

The role of CCL23, a ligand for the chemokine receptor CCR1, in tumorigenesis remains poorly understood. This study showed that CCL23 expression was frequently downregulated in liver cancer at mRNA and protein levels and associated with shortened patient survival, enrichment of signatures regarding cancer stem cell property, and metastatic potential. As CCL23 is a chemoattractant for various immune cells, it may cause the recruitment of immune cells into the tumor niche.[26,27] Our results indicated that CCL23 expression was associated with the tumor infiltration of $CD8^+$ T cells, thereby affecting patient outcomes. Similar effects on both tumor and immune cells are also observed for other CC chemokines. For instance, CCL2 could promote self-renewal by binding to CCR4 on prostate cancer cells and recruit M2-like tumor-associated macrophages and regulatory T cells to induce immune suppression.[28] CCL15 facilitates disease progression and immune escape in HCC by promoting tumor cells' metastatic potential in an autocrine fashion and recruiting $CCR1^+$ monocytes cells to the invasive margin.[29]

ESR1 is a potential tumor suppressor gene in several cancers. In breast cancer and non–small cell lung cancer, the expression level of ESR1 is noticeably downregulated.[30,31] In the context of cervical cancer, loss of ESR1 expression is associated with increased invasiveness and cancer progression.[32] ESR1 is also reported to be a candidate tumor suppressor gene in HCC. The decreased expression of ESR1 is related to high liver damage score, tumor size, and pathological invasion of the intrahepatic portal vein.[33] HCC patients with low ESR1 expression also had shorter survival.[34] As an oncogene, miR-9-5p fosters the proliferation, migration, and invasion of HCC cells by inhibiting ESR1 expression.[35] In contrast, overexpression of ESR1 suppressed proliferation and invasion, while induced apoptosis in liver cancer cells.[36,37] In this study, analysis of publicly available datasets and subsequent experiments confirmed our point of view that ESR1 could positively regulate the biogenesis of CCL23 by directly binding to its promoter region, inhibiting liver cancer progression at least partly by promoting the expression of CCL23.

AKT signaling plays a vital role in cancer stem cells, including the ability to maintain colony formation ability and proliferation.[38] Targeting the PI3K/AKT pathway could immensely reduce the bulk tumor burden and slow down the metabolism of cancer stem cells.[21,22] The PI3K/AKT pathway is also engaged in the development of liver cancer. Liu et al found Nrf2 could activate the AKT/p21 pathway, resulting in increased cell cycle progression of HCC cells.[23] Lu et al reported that miR-328-3p overexpression inhibited the PI3K/AKT pathway to attenuate the malignant proliferation and invasion of liver cancer.[39] A mechanism explaining the link between induction of AKT activation and concomitant repression of ERα activation is reported in breast cancer. Following the activation of AKT, the Forkhead box protein FOXO3a was phosphorylated and exported from the nucleus to the cytoplasm, where it was unable to activate the transcription of target genes, leading to decreased synthesis of ERα.[24,25] In the present work, our results demonstrate that CCL23 could suppress the activation of AKT and thus promote the expression of ESR1, inhibiting the progression of liver cancer.

In summary, our study elucidates that CCL23 is a potent tumor suppressor in liver cancer. Loss of CCL23 not only enhances stemness and metastasis initiation in an autocrine manner but also disturbs the recruitment of $CD8^+$ T cells to create an immunologically "cold" microenvironment in a paracrine fashion (Figure 6E). Targeting the ESR1/CCL23/CCR1/AKT feedback loop may provide a new therapeutic strategy and synergize with immunotherapy.

ACKNOWLEDGMENTS

This work was supported by the National Natural Science Foundation of China (No. 82060513, 82060297, 82060579, and 81902850), the Science and Technology Cooperation Program of Xinjiang Production and Construction Corps (2021BC002), the Youth Science and Technology Innovation Leading Talents Project of Xinjiang Production and Construction Corps (2020CB015), the Youth Innovation Talents Project of Shihezi University (CXBJ201907), and the Non-profit Central Research Institute Fund of Chinese Academy of Medical Sciences (2020-PT330-003).

DISCLOSURE

The authors have no conflict of interest.

ORCID

Lianghai Wang https://orcid.org/0000-0003-3128-7780

REFERENCES

1. Bray F, Ferlay J, Soerjomataram I, Siegel RL, Torre LA, Jemal A. Global cancer statistics 2018: GLOBOCAN estimates of incidence and mortality worldwide for 36 cancers in 185 countries. *CA Cancer J Clin*. 2018;68(6):394-424.
2. Fitzmaurice C, Abate D, Abbasi N, et al. Global, Regional, and National Cancer Incidence, Mortality, Years of Life Lost, Years Lived With Disability, and Disability-Adjusted Life-Years for 29 Cancer Groups, 1990 to 2017: A Systematic Analysis for the Global Burden of Disease Study. *JAMA Oncol*. 2019;5:1749-1768.

3. Tang A, Hallouch O, Chernyak V, Kamaya A, Sirlin CB. Epidemiology of hepatocellular carcinoma: target population for surveillance and diagnosis. *Abdom Radiol*. 2018;43:13-25.
4. Zucman-Rossi J, Villanueva A, Nault JC, Llovet JM. Genetic Landscape and Biomarkers of Hepatocellular Carcinoma. *Gastroenterology*. 2015;149(5):1226-1239.e4.
5. Zlotnik A, Yoshie O. Chemokines: a new classification system and their role in immunity.
6. Moser B, Wolf M, Walz A, Loetscher P. Chemokines: multiple levels of leukocyte migration control. *Trends Immunol*. 2004;25(2):75-84.
7. Zlotnik A, Yoshie O. Chemokines: a new classification system and their role in immunity. *Immunity*. 2000;12:121-127.
8. Moore BB, Arenberg DA, Stoy K, et al. Distinct CXC chemokines mediate tumorigenicity of prostate cancer cells. *Am J Pathol*. 1999;154:1503-1512.
9. Strieter RM, Polverini PJ, Arenberg DA, et al. Role of C-X-C chemokines as regulators of angiogenesis in lung cancer. *J Leukoc Biol*. 1995;57:752-762.
10. Müller A, Homey B, Soto H, et al. Involvement of chemokine receptors in breast cancer metastasis. *Nature*. 2001;410:50-56.
11. Wiley HE, Gonzalez EB, Maki W, Wu MT, Hwang ST. Expression of CC chemokine receptor-7 and regional lymph node metastasis of B16 murine melanoma. *J Natl Cancer Inst*. 2001;93:1638-1643.
12. Arakaki R, Yamasaki T, Kanno T, et al. CCL2 as a potential therapeutic target for clear cell renal cell carcinoma. *Cancer Med*. 2016;5:2920-2933.
13. Long H, Xie R, Xiang T, et al. Autocrine CCL5 signaling promotes invasion and migration of CD133+ ovarian cancer stem-like cells via NF-κB-mediated MMP-9 upregulation. *Stem cells*. 2012;30:2309-2319.
14. Zhu M, Xu W, Wei C, et al. CCL14 serves as a novel prognostic factor and tumor suppressor of HCC by modulating cell cycle and promoting apoptosis. *Cell Death Dis*. 2019;10:796.
15. Inoue K, Slaton JW, Eve BY, et al. Interleukin 8 expression regulates tumorigenicity and metastases in androgen-independent prostate cancer. *Clin Cancer Res*. 2000;6:2104-2119.
16. Bian X, Xiao YT, Wu T, et al. Microvesicles and chemokines in tumor microenvironment: mediators of intercellular communications in tumor progression. *Mol Cancer*. 2019;18:50.
17. Arya M, Patel HR, Williamson M. Chemokines: key players in cancer. *Curr Med Res Opin*. 2003;19:557-564.
18. Kawada K, Sonoshita M, Sakashita H, et al. Pivotal role of CXCR3 in melanoma cell metastasis to lymph nodes. *Can Res*. 2004;64:4010-4017.
19. Thorsson V, Gibbs DL, Brown SD, et al. The Immune Landscape of Cancer. *Immunity*. 2018;48(812–30):e14.
20. Hu H, Miao YR, Jia LH, Yu QY, Zhang Q, Guo AY. AnimalTFDB 3.0: a comprehensive resource for annotation and prediction of animal transcription factors. *Nucleic Acids Res*. 2019;47:D33-D38.
21. Kolev VN, Wright QG, Vidal CM, et al. PI3K/mTOR dual inhibitor VS-5584 preferentially targets cancer stem cells. *Can Res*. 2015;75:446-455.
22. Marhold M, Tomasich E, El-Gazzar A, et al. HIF1α regulates mTOR signaling and viability of prostate cancer stem cells. *Mol Cancer Res*. 2015;13:556-564.
23. Liu D, Zhang Y, Wei Y, et al. Activation of AKT pathway by Nrf2/PDGFA feedback loop contributes to HCC progression. *Oncotarget*. 2016;7:65389-65402.
24. Guo S, Sonenshein GE. Forkhead box transcription factor FOXO3a regulates estrogen receptor alpha expression and is repressed by the Her-2/neu/phosphatidylinositol 3-kinase/Akt signaling pathway. *Mol Cell Biol*. 2004;24:8681-8690.
25. Belguise K, Sonenshein GE. PKCtheta promotes c-Rel-driven mammary tumorigenesis in mice and humans by repressing estrogen receptor alpha synthesis. *J Clin Investig*. 2007;117:4009-4021.
26. Youn BS, Zhang SM, Broxmeyer HE, et al. Characterization of CKbeta8 and CKbeta8-1: two alternatively spliced forms of human beta-chemokine, chemoattractants for neutrophils, monocytes, and lymphocytes, and potent agonists at CC chemokine receptor 1. *Blood*. 1998;91:3118-3126.
27. Macphee CH, Appelbaum ER, Johanson K, et al. Identification of a truncated form of the CC chemokine CK beta-8 demonstrating greatly enhanced biological activity. *J Immunol*. 1950;1998(161):6273-6279.
28. Su W, Han HH, Wang Y, et al. The polycomb repressor complex 1 drives double-negative prostate cancer metastasis by coordinating stemness and immune suppression. *Cancer Cell*. 2019;36(139–55):e10.
29. Liu LZ, Zhang Z, Zheng BH, et al. CCL15 recruits suppressive monocytes to facilitate immune escape and disease progression in hepatocellular carcinoma. *Hepatology (Baltimore, MD)*. 2019;69:143-159.
30. Król MB, Galicki M, Grešner P, et al. The ESR1 and GPX1 gene expression level in human malignant and non-malignant breast tissues. *Acta Biochim Pol*. 2018;65:51-57.
31. Aresti U, Carrera S, Iruarrizaga E, et al. Estrogen receptor 1 gene expression and its combination with estrogen receptor 2 or aromatase expression predicts survival in non-small cell lung cancer. *PLoS ONE*. 2014;9:e109659.
32. Zhai Y, Bommer GT, Feng Y, Wiese AB, Fearon ER, Cho KR. Loss of estrogen receptor 1 enhances cervical cancer invasion. *Am J Pathol*. 2010;177:884-895.
33. Hishida M, Nomoto S, Inokawa Y, et al. Estrogen receptor 1 gene as a tumor suppressor gene in hepatocellular carcinoma detected by triple-combination array analysis. *Int J Oncol*. 2013;43:88-94.
34. Wang X, Liao X, Huang K, et al. Clustered microRNAs hsa-miR-221-3p/hsa-miR-222-3p and their targeted genes might be prognostic predictors for hepatocellular carcinoma. *J Cancer*. 2019;10:2520-2533.
35. Wang L, Cui M, Cheng D, et al. miR-9-5p facilitates hepatocellular carcinoma cell proliferation, migration and invasion by targeting ESR1. *Mol Cell Biochem*. 2021;476(2):575-583.
36. Tu CC, Kumar VB, Day CH, et al. Estrogen receptor α (ESR1) overexpression mediated apoptosis in Hep3B cells by binding with SP1 proteins. *J Mol Endocrinol*. 2013;51:203-212.
37. Deng L, Yang H, Tang J, et al. Inhibition of MTA1 by ERα contributes to protection hepatocellular carcinoma from tumor proliferation and metastasis. *J Exp Clin Cancer Res*. 2015;34:128.
38. Zhou J, Wulfkuhle J, Zhang H, et al. Activation of the PTEN/mTOR/STAT3 pathway in breast cancer stem-like cells is required for viability and maintenance. *Proc Natl Acad Sci USA*. 2007;104:16158-16163.
39. Lu H, Hu J, Li J, Lu W, Deng X, Wang X. miR-328-3p overexpression attenuates the malignant proliferation and invasion of liver cancer via targeting Endoplasmic Reticulum Metallo Protease 1 to inhibit AKT phosphorylation. *Ann Transl Med*. 2020;8:754.

SUPPORTING INFORMATION

Additional supporting information may be found online in the Supporting Information section.

How to cite this article: Meng J, Wang L, Hou J, et al. CCL23 suppresses liver cancer progression through the CCR1/AKT/ESR1 feedback loop. *Cancer Sci*. 2021;112:3099–3110. https://doi.org/10.1111/cas.14995